DISCLAIMER

This document was prepared as an account of work sponsored by the United States Government. While this document is believed to contain correct information, neither the United States Government nor any agency thereof, nor The Regents of the University of California, nor any of their employees, makes any warranty, express or implied, or assumes any legal responsibility for the accuracy, completeness, or usefulness of any information, apparatus, product, or process disclosed, or represents that its use would not infringe privately owned rights. Reference herein to any specific commercial product, process, or service by its trade name, trademark, manufacturer, or otherwise, does not necessarily constitute or imply its endorsement, recommendation, or favoring by the United States Government or any agency thereof, or The Regents of the University of California. The views and opinions of authors expressed herein do not necessarily state or reflect those of the United States Government or any agency thereof or The Regents of the University of California.

Gas-Phase Oxidation of Cm^+ and Cm^{2+}—Thermodynamics of neutral and ionized CmO

John K. Gibson [a,*], Richard G. Haire [b], Marta Santos [c], António Pires de Matos [c], and Joaquim Marçalo [c,*]

[a] Chemical Sciences Division, Lawrence Berkeley National Laboratory, Berkeley, CA 94720, USA

[b] Chemical Sciences Division, Oak Ridge National Laboratory, Oak Ridge, TN 37831, USA

[c] Departamento de Química, Instituto Tecnológico e Nuclear, 2686-953 Sacavém, Portugal

[*] Corresponding authors. Email: JKGibson@lbl.gov (J.K.G.); jmarcalo@itn.pt (J.M.)

Keywords: curium; actinides; lanthanides; ionization energy; bond energy; FTICR/MS

Abstract

Fourier transform ion cyclotron resonance mass spectrometry was employed to study the products and kinetics of gas-phase reactions of Cm^+ and Cm^{2+}; parallel studies were carried out with $La^{+/2+}$, $Gd^{+/2+}$ and $Lu^{+/2+}$. Reactions with oxygen-donor molecules provided estimates for the bond dissociation energies, $D(M^+\text{-}O)$ (M = Cm, Gd, Lu). The first ionization energy, IE(CmO), was obtained from the reactivity of CmO^+ with dienes, and the second ionization energies, $IE(MO^+)$ (M = Cm, La, Gd, Lu), from the rates of electron-transfer reactions from neutrals to the MO^{2+} ions. The following thermodynamic

quantities for curium oxide molecules were obtained: IE(CmO) = 6.4±0.2 eV; IE(CmO^+) = 15.8±0.4 eV; D(Cm-O) = 710±45 kJ mol^{-1}; D(Cm^+-O) = 670±40 kJ mol^{-1}; and D(Cm^{2+}-O) = 342±55 kJ mol^{-1}. Estimates for the M^{2+}-O bond energies for M = Cm, La, Gd and Lu are all intermediate between D(N_2-O) and D(OC-O)—i.e., 167 kJ mol^{-1} < D(M^{2+}-O) < 532 kJ mol^{-1}—such that the four MO^{2+} ions fulfill the thermodynamic requirement for catalytic O-atom transport from N_2O to CO. It was demonstrated that the kinetics are also favorable and that the CmO^{2+}, LaO^{2+}, GdO^{2+} and LuO^{2+} dipositive ions each catalyze the gas-phase oxidation of CO to CO_2 by N_2O. The CmO_2^+ ion appeared during the reaction of Cm^+ with O_2 when the intermediate, CmO^+, was not collisionally cooled—although its formation is kinetically and/or thermodynamically unfavorable, CmO_2^+ is a stable species.

Introduction

Reactions and thermodynamics of elementary gas-phase species enable a better understanding of various fundamental aspects of 5f molecular chemistry, as well as provide a basis for developing and validating advanced theoretical methodologies for molecular systems incorporating actinides (1,2). Such experimental results are also essential for developing advanced technologies and applications in the nuclear industry, and for predicting and/or controlling the behavior of actinides in the environment.

Very little thermodynamic information is available for even elementary binary curium oxide molecules (3,4). Smith and Peterson (5) performed a seminal study of the high-temperature vaporization of Cm_2O_3(s) and estimated D(Cm-O) ≈ 728 kJ mol^{-1}; although no subsequent quantitative measurements of the dissociation energy of

curium monoxide have been reported, recent experiments on the vaporization of curium oxide solids are in accord with these early results (6,7). Konings has summarized the thermodynamic information available for curium, including an estimate for the enthalpy of formation of CmO(g) (8). Other than the bond energy for CmO provided by Smith and Peterson (5), there is essentially no experimental thermodynamic information available for curium oxide molecules; a key goal of the present study was to rectify this deficiency. A recent theoretical study of CmO and CmO_2 (9) provided estimates for D(Cm-O) and D(OCm-O); however, without additional experimental validation of the theoretical methodologies employed for actinide-containing molecules, the reliability of such computed bond energies for heavy element molecules remains uncertain.

We have previously employed Fourier transform ion cyclotron resonance mass spectrometry (FTICR/MS) to study oxidation reactions of $Pa^{+/2+}$, $Np^{+/2+}$, $Pu^{+/2+}$, and $Am^{+/2+}$ (10-14). In that work, bond dissociation energies, $D(M^{+/2+}\text{-O})$ and/or $D(OM^{+/2+}\text{-O})$, were estimated from the observed oxidation reactions, and ionization energies, $I(MO^{0/+})$ and/or $I(MO_2^{0/+})$, were obtained from either electron-transfer reactions, or reactions with dienes (15). In the present work, we extended these studies to the next member of the actinide series, curium. Studies with representative lanthanide ions, particularly $Gd^{+/2+}$ (the 4f electron counterpart of Cm) and $Lu^{+/2+}$, were carried out for comparison with the results for $Cm^{+/2+}$. Aspects of the chemistry of these metal ions are evaluated in the framework of their atomic energetics—the ground state configurations for Cm^+, Gd^+ and Lu^+ are given in Table 1, together with the promotion energies for attaining divalent state configurations, as well as the second ionization energies.

Experimental

The experimental details have been provided elsewhere (10-14,19,20) and only a brief summary is included here. Ions were produced by laser desorption/ionization (LDI) using the fundamental 1064 nm wavelength of a Spectra-Physics Quanta-Ray GCR-11 Nd:YAG laser. The LDI targets were dilute alloys of the f-block metal in platinum. For example, the curium target was ~5 at% Cm in Pt. The curium-248 isotope used in this work, produced in the high-flux isotope reactor at ORNL; it has an alpha emission half life of 3.5×10^5 y.

Ions emitted from the targets by LDI entered the source cell of a Finnigan FT/MS 2001-DT FTICR/MS equipped with a 3T magnet and controlled by a Finnigan Venus Odyssey data system; all experiments were carried out in the source cell. With the exception of CH_2O, which was prepared according to a literature procedure (21), the reactant gases were commercial products. The purities of the gases were confirmed to be >99% from electron ionization mass spectra. The gases were introduced into the spectrometer through a leak valve to pressures of ca. 10^{-8} to 10^{-7} Torr; for some experiments, an initial oxidation step was accomplished by an oxidant gas introduced though pulsed valves. Pressures were measured with a calibrated (22-25) Bayard-Alpert type ionization gauge. Isolation of the reactant ions was achieved by ejection of other ions using single-frequency, frequency sweep, or SWIFT excitation (26). Unless otherwise noted, the reactant ions were cooled by collisions with argon, and their thermalization was confirmed by reproducibility of reaction kinetics and product distributions, as well as by the linearity of the pseudo-first-order reactant ion decay plots.

Pseudo first-order reaction rate constants, k, were determined from the decay of the reactant ion signals as a function of time at constant neutral reagent pressures. Each reaction was studied for sufficiently long reaction times that less than 10% of the reagent ion remained; the linearity of the kinetic plots over this range established that the ion population was effectively thermalized. Reaction efficiencies are reported as k/k_{COL}, where k_{COL} is the collisional rate constant derived from the modified variational transition-state/classical trajectory theory of Su and Chesnavich (27). Uncertainties of ±50% are assigned to the absolute rate constants; relative uncertainties in the reported rate constants, k and k/k_{COL}, are estimated as ±20%.

Results and Discussion

Reactions of M^+ and MO^+ with oxidants: An evaluation of $D(Cm^+\text{-}O)$

The bare and oxo-ligated metal ions, M^+ and MO^+ where M = Cm, Gd or Lu, were reacted with several oxidants under bimolecular reaction conditions. Under the low-energy conditions of these experiments, if an oxidation or other reaction is observed it must be exothermic (or thermoneutral)—i.e., $\Delta_r H \geq 0$. Accordingly, the occurrence of a reaction can be used to establish a lower thermodynamic limit. For some reactions there may a direct correlation between reaction efficiencies and the degree of exothermicity, but such a correspondence is not necessarily general. Furthermore, non-observation of a reaction may be due to inefficient kinetics and therefore does not necessarily indicate that the absent reaction is endothermic. However, as discussed below, in some cases it is reasonable to infer thermodynamic information based on non-observation of certain reactions. The several oxidants, "RO", used in the present

work exhibit a range of bond energies, BDE(R-O), and reactivities which are appropriate for evaluating the thermodynamics of f-block metal ion oxidation reactions.

The results for reactions of M^+ ions with oxidants are summarized in Table 2. The bond energies and ionization energies of the oxidants are given in Table 3. The reactivity of Gd^+ and Lu^+ (and other lanthanide cations) with several oxidants—N_2O (30), O_2 (30), NO (31), D_2O (32), and CO_2 (33)—have been previously studied by Bohme and co-workers using an inductively coupled plasma/selected-ion flow tube (ICP/SIFT) tandem mass spectrometer, with concurrent results.

As observed reactions must be exothermic (or thermoneutral) under low-energy experimental conditions, these oxidation reactions establish the following lower limits for the M^+-O bond energies: $D(Cm^+\text{-}O) \geq D(N\text{-}O) = 631.6$ kJ mol^{-1}; $D(Gd^+\text{-}O) \geq D(H_2C\text{-}O) = 751.5$ kJ mol^{-1}; and $D(Lu^+\text{-}O) \geq D(OC\text{-}O) = 532.2$ kJ mol^{-1}. The literature values for $D(Gd^+\text{-}O) = 732\pm15$ kJ mol^{-1} and $D(Lu^+\text{-}O) = 520\pm15$ kJ mol^{-1} (34) are slightly below these new lower limits; there is no experimental value for $D(Cm^+\text{-}O)$.

In contrast to the requirement of exothermicity for the occurrence of an ion-neutral reaction, the non-observation of an oxidation reaction may alternatively be due to kinetic hindrance factors and thus does not necessarily indicate endothermicity and does not a priori establish an upper limit for the bond energy. However, previous studies regarding metal ion oxidation with the same oxidants as employed here have indicated some generalizations can be inferred regarding the kinetics for oxygen-atom transfers to metal ions (10,11). In particular, oxidations by N_2O, H_2O, and CO_2 often exhibit substantial activation barriers; in contrast, C_2H_4O, O_2, NO, and CH_2O are generally relatively facile oxygen-atom donors. Accordingly, from the experimental

results we tentatively propose the following upper limits: $D(Cm^+-O) \leq D(H_2C-O) = 751.5$ kJ mol^{-1}; and $D(Lu^+-O) \leq D(N-O) = 631.6$ kJ mol^{-1}. Furthermore, the observation that oxidation of Cm^+ by NO proceeds quite inefficiently (see Table 2) suggests this reaction is within <100 kJ mol^{-1} of the thermodynamic threshold of 631.6 kJ mol^{-1}. Accordingly, we estimate $D(Cm^+-O) = 670\pm40$ kJ mol^{-1}. Considering the previous literature values (34), as well as the kinetics measured in the present work, we also arrive at the following estimates: $D(Gd^+-O) = 780\pm30$ kJ mol^{-1}; and $D(Lu^+-O) = 560\pm30$ kJ mol^{-1}.

Under thermal conditions, both CmO^+ and GdO^+ were unreactive towards N_2O, O_2, CO_2, NO and CH_2O; LuO^+ was unreactive with the first three of these oxidants (the reactions of LuO^+ with NO and CH_2O were not studied). As the highest common oxidation state for Cm, Gd and Lu is M(III), it is not surprising that oxidation does not readily occur to the MO_2^+, in which the formal oxidations states would be assigned as M(V). With H_2O, each of the three MO^+ exhibited inefficient addition reactions to give $CmO_2H_2^+$, $GdO_2H_2^+$ and $LuO_2H_2^+$. These addition products may be adducts, $MO^+\bullet H_2O$, or bis-hydroxides, $M(OH)_2^+$, where the trivalent oxidation states of the metal centers are retained. Reactions of the MO^+ with ethylene oxide revealed distinctive behaviors discussed below.

Although oxidation of CmO^+ did not occur after collisionally cooling, oxidation to CmO_2^+ by O_2 did occur in the Cm^+/O_2 reaction sequence when the CmO^+ intermediate was not thermalized. This observation can be attributed to the oxidation of a nascent excited state CmO^+, denoted as CmO^{+*}, according to Equations (1a) and (1b).

$$Cm^+ + O_2 \rightarrow CmO^{+*} + O \quad (1a)$$

$$CmO^{+*} + O_2 \rightarrow CmO_2^+ + O \qquad (1b)$$

As the secondary CmO_2^+ product appears only in the absence of cooling of the intermediate CmO^{+*}, Equation (1b) is evidently thermodynamically and/or kinetically hindered under thermal conditions. The occurrence of Equation (1b) demonstrates that CmO_2^+ is an intrinsically stable species which evidently resides at a local energy minimum on the potential energy surface.

Reactions of MO^+ with dienes: Evaluations of IE(CmO) and D(Cm-O)

Cornehl et al. (15) identified a correlation between the electron affinities of LnO^+ ($EA(LnO^+)$) and the efficiencies of these ions in activation of 1,3-butadiene (C_4H_6) and isoprene (C_5H_8). The correlation was presented in the framework of IE(LnO), which are equivalent to $EA(LnO^+)$ and thus the electrophilicities of the metal oxide ions. It was subsequently established that a similar behavior appeared for AnO^+ with these dienes: the greater the IE(AnO), the more efficient the reaction with a given diene substrate (11). Although the same correlation of reactivity with $EA(MO^+)$ was exhibited within both the lanthanide and actinide series, evidently there is a "reactivity offset" between the two series such that for LnO^+ and AnO^+ ions with similar EAs, the absolute reactivity of the LnO^+ ion is greater than that of the AnO^+ ion. In particular, the onset of reactivity with isoprene appears for TbO^+ (EA ≈ 5.6 eV) among the LnO^+ ions (15), and for UO^+ (EA = 6.03 eV (35)) among the AnO^+ ions (11). The evident requirement for a higher EA for the actinide oxide ions may reflect the generally greater covalent contribution to bonding in actinide complexes (36). Such a greater covalency should reduce the effective charge on the metal center, thereby generally diminishing the efficacy of electrophilic attack of AnO^+ ions compared with more ionic LnO^+ ions.

Because the ThO^+ ion distinctively produces the radical-like $ThOC_5H_5^+$ product in its reaction with isoprene (11), the reactivity of UO^+ with dienes is considered to better represent the characteristic electrophilic attack mechanism seen with the LnO^+ (37). Accordingly, IE(UO) = 6.0313±0.0006 eV (35) is used as the benchmark for evaluating the IE(AnO) based on reactivities of AnO^+ with dienes (11,12). The results for reactions of CmO^+ with dienes are given in Table 4. Other than inefficient adduct formation with ThO^+ (11) and significant reactivity with PaO^+, which constitutes a special case in the An series (37), no other AnO^+ ions (An = U, Np, Pu, Am, Cm) reacted with butadiene (11). The reaction efficiencies with isoprene ranged from k/k_{COL} = 0.01 for NpO^+ and PuO^+ (11), up to 0.19 for CmO^+ as measured in the present work. Although the reaction efficiency of UO^+ with isoprene (k/k_{COL} = 0.02 (11)) was apparently slightly greater than for NpO^+ and PuO^+, dehydrogenation was induced by the latter two ions whereas UO^+ exhibited only adduct formation: thus, the intrinsic reactivity of UO^+ is considered slightly lower than of NpO^+ and PuO^+. The overall order of AnO^+ reactivities with dienes is assigned as follows, with the IE(MO)/eV given in parentheses:

ThO^+ (6.60) > CmO^+ (6.4±0.2) > AmO^+(6.2±0.2) > NpO^+ (6.1±0.2) ≈ PuO^+ (6.1±0.2) ≥ UO^+ (6.03)

The values for IE(ThO) and IE(UO) are from Heaven and coworkers (35,38); the IE(AmO), IE(NpO) and IE(PuO) were obtained previously from diene reactivities (11,12). The assigned IE(CmO) = 6.4 ±0.2 eV is based on the observation that both CmO^+ and AmO^+ are inert towards butadiene but the reactivity with isoprene is greater for CmO^+ (k/k_{COL} = 0.19) than AmO^+ (k/k_{COL} = 0.04 eV (11)). This new estimate for IE(CmO) = 6.4±0.2 eV is in accord with a qualitative prediction (39) that IE(CmO) > IE(Cm) = 5.9914 eV (40).

Although the comparative reactivity of ThO^+ was not used as a benchmark per se, inclusion of its reactivity in the present evaluation is consistent with the comparative ionization energies. In a recent theoretical study (9), IE(AmO) = 6.3 eV was obtained, in good agreement with the experimental value, 6.2±0.2 eV, previously obtained using the diene reactivity method (11,12).

Using the $D(CmO^+)$ = 670±40 kJ mol^{-1} estimated above, IE(CmO) = 6.4±0.2 eV, and IE(Cm) = 5.9914 eV (40), we obtain $D(CmO) = D(CmO^+)$ - IE(Cm) + IE(CmO) = 710 ± 45 kJ mol^{-1}. This value is in good agreement with the value of 728 kJ mol^{-1} reported by Smith and Peterson (5), as well as with a more recent estimate of 709 kJ mol^{-1} (41). Konings (8) has presented thermodynamic estimates for curium and its oxides. Using $\Delta H_f(Cm(g))$ = 384±10 kJ mol^{-1} and $\Delta H_f(CmO(g)) \approx$ -175 kJ mol^{-1} from ref. (8), and $\Delta H_f(O(g))$ = 249 kJ mol^{-1} (28), $D(CmO) \approx$ 808 kJ mol^{-1} is derived, which is ~100 kJ mol^{-1} higher than the value deduced from our experimental results; accordingly, we suggest that the actual value for $\Delta H_f(CmO(g))$ may be less negative than -175 kJ mol^{-1} (8). A recent theoretical treatment (9) provided a computed value of D(Cm-O) = 685 kJ mol^{-1}, which is in rather good agreement with our experimental value of 710±45 kJ mol^{-1}.

Results for the reactions of GdO^+ and LuO^+ with dienes are included in Table 4. Our results are in qualitative accord with those for LuO^+/butadiene and GdO^+/isoprene from Cornehl et al. (15)—in particular, the reactivity of LuO^+ was substantially greater than that of GdO^+. However, our k/k_{COL} values are evidently approximately four times lower than those reported previously (15). Given this discrepancy, it should be emphasized that our evaluations employ reaction efficiencies obtained under internally consistent experimental conditions, and the relative values are considered accurate to

within ±20%. In the case of LuO^+/butadiene, we did not observe adduct formation as reported previously (15), but rather H_2-elimination, which is in accord with the high reactivity of LuO^+ towards this substrate.

Results for reactions of the bare Cm^+ ion with butadiene and isoprene are also included in Table 4. These reaction efficiencies with the dienes are intermediate between those reported previously (11,37) for the highly reactive early actinide ions, Th^+, Pa^+, U^+ and Np^+, and the less reactive Pu^+ ion. These comparative reactivities accord with the promotion energy for Cm^+ to the $5f^76d7s$ reactive state for hydrocarbon activation, as has been discussed in detail previously (37) (the pertinent promotion energy for Cm^+ is included in Table 1).

Reactions of MO^+ with ethylene oxide

Each of the three MO^+ dehydrogenated C_2H_4O to produce $MO_2C_2H_2^+$ (M = Cm, Gd, Lu); $LuOCH_2^+$ was also produced as a minor (15%) product. The following reaction efficiencies, k/k_{COL}, were measured, with the absolute rate constants, $k/10^{-10}$ cm^3 $molecule^{-1}$ s^{-1}, given in brackets: CmO^+ / 0.15 (2.58); GdO^+ / 0.067 (1.18); LuO^+ / 0.34 (5.88). For comparison, k/k_{COL} = 0.03 was previously reported for the reaction of AmO^+ with C_2H_4O, with the dominant (60%) channel also being dehydrogenation to give $AmO_2C_2H_2^+$ (11). Other AnO^+ (An = Th, Pa, U, Np, Pu) (10,14) did not dehydrogenate C_2H_4O, but instead were oxidized to the AnO_2^+ ions. Thus, the following comparative H_2-elimination reaction efficiencies were identified for ethylene oxide: $CmO^+ > AmO^+$; and $LuO^+ > GdO^+$. These are the same orderings as exhibited with dienes and, as discussed above, parallel the EA(MO^+) = IE(MO).

The apparent correlation between the MO^+ reaction efficiencies for dienes and ethylene oxide suggests a correspondence between the two reaction mechanisms. For dienes, the proposed mechanism entails electrophilic attack of the MO^+ on the π-electron systems (15). The IEs of different dienes should be qualitatively indicative of their relative nucleophilicities: the lower the IE of a diene, the greater its electron-donating capability and thus the greater its nucleophilicity. However, as Cornehl et al. (15) remarked, this is somewhat of an oversimplification: "…ionization energies cannot be regarded as a quantitative measure of their nucleophilicity." (15).

An alternative, perhaps more direct, measure of the nucleophilicity of a molecule is its proton affinity (PA). Ionization energies and proton affinities for some molecules are given in Table 5. It is apparent that small dienes and monoenes exhibit an inverse correlation between IE and PA, so their IEs do indeed provide a qualitative indication of relative nucleophilicities for these similar molecules. In a previous study (37), it was found that AmO^+ and CmO^+ do not activate ethylene, propene or 1-butene, which is consistent with the greater IEs and lower PAs of the monoenes as compared with the dienes (Table 5), and thus their lower nucleophilicities.

We propose that the reactions of the MO^+ with ethylene oxide proceed by a mechanism in which the rate-determining step entails electron donation from ethylene oxide to the MO^+—the observed dependence on IE(MO) would be a consequence of this. It is apparent from the IEs and PAs for substrates such as ethylene oxide and water (Table 5) that the IEs do not consistently parallel the PAs, and thus the IEs do not provide a general measure of nucleophilicity. In particular, the IE of ethylene oxide is much greater than that of 1,3-butadiene, but their PAs are quite similar. As remarked by

Cornehl et al. (15), the particular interaction between an electrophilic MO^+ ion and a nucleophilic neutral substrate will determine the potential energy surface and thus the reaction efficiency. The observation that the MO^+ ions react with ethylene oxide at a comparable efficiency as with the more nucleophilic isoprene substrate—see the PAs in Table 5—suggests different reaction mechanisms apply for ethylene oxide and dienes, as expected from ab initio considerations. In contrast to an electrophilic attack of the diene π-system, a key characteristic of the initial association complex of the MO^+ with C_2H_4O is probably interaction of the oxophilic metal center with the bridging oxo in the neutral molecule, perhaps in concert with electron donation from the neutral C_2H_4O molecule to the MO^+ ion.

For reactions of butadiene with lanthanide oxide ions, it was postulated (15) that the MO^+ ions (M = Ln) add across the terminal carbons to produce a metalla-oxa-cyclohexene intermediate, *cyclo*{-CH_2-CH=CH-CH_2-M^+-O-}, which eliminates H_2 to produce a metalla-oxa-cyclohexadiene product, *cyclo*{-CH=CH-CH=CH-M^+-O-}. Given the oxophilicity of the metal center, the reaction of an MO^+ with ethylene oxide may proceed by insertion of MO^+ ions into a C-O bond as by a mechanism such as shown in Scheme 1. The initial association complex **1** might produce the metalla-dioxa-cyclopentane **3**, *cyclo*{-CH_2-CH_2-O-M^+-O-}, via some indeterminate intermediate(s) as roughly represented by structure **2**. Finally, H_2-elimination from **3** could produce a metalla-dioxa-cyclopentene product **4**, *cyclo*{-CH=CH-O-M^+-O-}. Collision induced dissociation (CID) of $LuO_2C_2H_2^+$ resulted in the following fragmentation products: $LuO_2C_2^+$ (i.e., loss of H_2), $LuOCH_2^+$ (loss of CO), LuO^+ (loss of C_2H_2O), and bare Lu^+.

Although these CID results do not provide direct evidence for the postulated metalla-dioxa-cyclopentene, structure **4** in Scheme 1, they are consistent with it.

Reactions of M^{2+} ions with oxidants

The ground state valence electron configurations of the dipositive metal ions are: $5f^8$ for Cm^{2+}, 5d for La^{2+}, $4f^7 5d$ for Gd^{2+}, and $4f^{14}6s$ for Lu^{2+} (16,17). For each of these M^{2+} ions, the lowest-lying reactive state with two non-f valence electrons is $f^{n-2}d^2$, with the promotion energies to these states estimated as >7 eV (42). In view of these high promotion energies to a prepared divalent bonding state for the M^{2+} ions, it is expected that the bonds in M^{2+}-O should be much weaker those in M^+-O (the lower promotion energies for the M^+ ions are given in Table 1). Accordingly, the M^{2+} ions were found to be more resistant to oxidation as compared with the M^+ ions.

The results for reactions of the M^{2+} ions with oxidants are summarized in Table 6 (the results for the La^{2+}/N_2O reaction are included as a footnote there). The four M^{2+} ions (M = Cm, La, Gd, Lu) were oxidized to MO^{2+} ions by N_2O. The electronic structures of these MO^{2+} ions are intriguing, as the metal center would be in an unusual, formally tetravalent oxidation state in the "M^{2+}=O" species. While a Cm(IV) state is known, this oxidation state is not known for the 4f elements investigated here. The implication of oxidation by N_2O is that $D(M^{2+}\text{-}O) \geq 167.1$ kJ mol^{-1} for all four M^{2+}, in accord with the thermodynamic assessment below. The result that none of the other oxidants produced MO^{2+} ions (M = Cm, Gd, Lu) is also in accord with our estimates below for $D(M^{2+}\text{-}O)$.

With C_2H_4O, the three M^{2+} ions (M = Cm, Gd, Lu) were oxidized concomitant with electron-transfer, to produce MO^+. The generic reaction for such an

oxidation/electron-transfer is given by Eqn. (2a), and the associated enthalpy by Eqn. (2b):

$$M^{2+} + RO \rightarrow MO^{+} + R^{+} \qquad (2a)$$

$$\Delta H((2a)/M) = D(R\text{-}O) - D(M^{+}\text{-}O) - IE(M^{+}) + IE(R) \qquad (2b)$$

Using the $D(M^{+}\text{-}O)$ values estimated above, 670±40 kJ mol^{-1} for Cm, 780±30 kJ mol^{-1} for Gd, and 560±30 kJ mol^{-1} for Lu; $D(O\text{-}C_2H_4)$ = 354.3 kJ mol^{-1} (28); $IE(C_2H_4)$ = 10.51 eV (29); and the $IE(M^{+})$ values given in Table 1, we obtain the following enthalpies from Eqn. (2b) for $RO = C_2H_4O$,: $\Delta H((2a)/Cm) \approx$ -498 kJ mol^{-1}; $\Delta H((2a)/Gd) \approx$ -578 kJ mol^{-1}; and $\Delta H((2a)/Lu) \approx$ -533 kJ mol^{-1}. Each of the three observed oxidation/charge separation reactions is quite exothermic. Despite the fact that $IE(Cm^{+})$ and $IE(Gd^{+})$ are 1.9 eV and 1.5 eV above $IE(C_2H_4O)$, simple electron transfers to give these bare M^{+} ions were not observed; instead, the much more exothermic oxidation/electron transfer reactions, Eqn. (2a), were overwhelmingly dominant. In contrast, $IE(Lu^{+})$ is fully 3.3 eV above $IE(C_2H_4O)$ and accordingly electron transfer to Lu^{2+} was sufficiently exothermic that it was observed as an alternative reaction pathway (see Table 3).

It is notable that electron transfer from N_2 did not occur upon oxidation of the M^{2+} ions by N_2O. Evaluation of Eqn. (2b) for $RO = N_2O$ (using the $D(N_2\text{-}O)$ in Table 2 and $IE(N_2)$ = 15.58 eV (29)) gives the following approximate enthalpies for formation of $\{MO^{+} + N_2^{+}\}$: $\Delta H((2a)/Cm) \approx$ -196 kJ mol^{-1}; $\Delta H((2a)/Gd) \approx$ -276 kJ mol^{-1}; and $\Delta H((2a)/Lu) \approx$ -231 kJ mol^{-1}. That these exothermic charge-separation exit channels were not observed may be due to activation barriers analogous to those which occur during electron transfer from a neutral to a dipositive ion (43), which can be understood in terms of

Coulombic repulsion between the two emerging monopositive product ions during dissociation of the dipositive encounter complex.

The formation of MOH^{2+} from the M^{2+}/H_2O reactions indicates strong metal hydroxide bonds: $D(M^{2+}\text{-}OH) \geq D(H\text{-}OH) = 498$ kJ mol^{-1} (28) (M = Cm, Gd, Lu). In view of kinetic considerations discussed above, the fact that the charge-separation channel, $\{MOH^+ + H^+\}$, was not observed does not necessarily imply that $IE(MOH^+) \leq IE(H) = 13.60$ eV (29).

For the reactions of M^{2+} with O_2 (using the D(O-O) in Table 2 and IE(O) = 13.62 eV (29)), Eqn. (2a) should be somewhat exothermic, by about -54 kJ mol^{-1} for Cm, about -134 kJ mol^{-1} for Gd, and about -89 kJ mol^{-1} for Lu. None of these three M^{2+} ions exhibited detectable reactivity with O_2, suggesting the presence of an activation barrier. The analogous evaluation for the M^{2+}/CO_2 reactions using Eqn. (2b) (using the D(OC-O) and IE(CO) in Table 1) suggests that the non-observed reactions to produce $\{MO^+ + CO^+\}$ are close to being thermoneutral: $\Delta H((2a)/Cm) \approx 18$ kJ mol^{-1}; $\Delta H((2a)/Gd) \approx -62$ kJ mol^{-1}; $\Delta H((2a)/Lu) \approx -17$ kJ mol^{-1}. With NO, both oxidation reactions—to $\{MO^{2+} + N\}$ and to $\{MO^+ + N^+\}$—should be endothermic for Cm, Gd and Lu, and these reactions are not observed experimentally. Instead, electron transfers from NO to the M^{2+} ions are exothermic by ≥ 2.8 eV and occur efficiently for all three M^{2+}.

The reaction pathways for the M^{2+} ions with CH_2O are more diverse due to charge-separation channels enabled by the low ionization energies of the O-atom and H-atom donor by-products: $IE(CH_2) = 10.40$ eV and IE(CHO) = 8.12 eV (29). The enthalpies estimated from the charge-separation oxidation reaction, Eqn. (2a), for RO = CH_2O are as follows: $\Delta H((2a)/Cm) \approx -111$ kJ mol^{-1}; $\Delta H((2a)/Gd) \approx -191$ kJ mol^{-1}; and

$\Delta H((2a)/Lu) \approx -146$ kJ mol^{-1}. Evidently, formation of CmO^+ by Eqn. (2a) with RO = CH_2O is sufficiently exothermic that it occurs, albeit rather inefficiently. As expected from the reaction enthalpies cited above, the formation of GdO^+ is more facile. The alternative hydride-transfer channels appear for the Gd^{2+} and Lu^{2+}ions, but not for the Cm^{2+} ion. The hydride-transfer reaction is given by Eqn. (3a) and its enthalpy by Eqn. (3b); IE(CHO) = 8.12 eV (29) and D(H-CHO) = 372 kJ mol^{-1} (28) have been incorporated:

$$M^{2+} + CH_2O \rightarrow MH^+ + CHO^+ \qquad (3a)$$

$$\Delta H((3a)/M) = D(H\text{-}CHO) - D(M^+\text{-}H) - IE(M^+) + IE(CHO) = 1155 \text{ kJ mol}^{-1} - D(M^+\text{-}H) - IE(M^+) \qquad (3b)$$

Elkind et al. (44) have reported $D(Lu^+\text{-}H) = 204\pm15$ kJ mol^{-1}, from which $\Delta H((3a)/Lu) \approx -390$ kJ mol^{-1} is obtained; this exothermic channel is observed. Values for $D(Cm^+\text{-}H)$ and $D(Gd^+\text{-}H)$ have not been reported and are unspecified in the following: $\Delta H((3a)/Cm) = -40 \text{ kJ mol}^{-1} - D(Cm^+\text{-}H)$; $\Delta H((3a)/Gd) = -11 \text{ kJ mol}^{-1} - D(Gd^+\text{-}H)$. As the reaction given by Eqn. (3a) is observed for Gd, it is inferred that $D(Gd^+\text{-}H)$ is sufficiently large to drive the reaction. It might be inferred that $D(Cm^+\text{-}H)$ is in contrast not sufficiently large, and perhaps $D(Cm^+\text{-}H) < D(Gd^+\text{-}H)$. The ground state of Cm^+ is quasi-closed-shell singlet $5f^77s^2$ (Table 1) and promotion—e.g., to $5f^76d7s$—is required to form even a two-electron covalent bond, as in a hydride. In contrast, the ground state of Gd^+ is already $4f^75d6s$, suitable for formation of a Gd^+-H bond. The higher promotion energy for Cm^+ may alternatively manifest itself as presenting a kinetic hindrance in hydride-transfer reactions. Finally, $IE(Lu^{2+}) = 13.90$ eV is sufficiently higher than $IE(CH_2O) = 10.88$ eV such that efficient electron-transfer occurs to produce bare Lu^+ (+ CH_2O^+).

Each of the MOH^{2+} primary products of the M^{2+}/H_2O reactions (M = Cm, Gd, Lu) reacted efficiently with a second H_2O molecule to give MO^+ according to Eqn. (4):

$$MOH^{2+} + H_2O \rightarrow MO^+ + H_3O^+ \qquad (4)$$

The measured efficiencies, k/k_{COL}, and absolute rates, ($k/10^{-10}$ cm^3 $molecule^{-1}$ s^{-1}), for these proton-transfer reactions were as follows: $CmOH^{2+}$ / 0.57 (24.78); $GdOH^{2+}$ / 0.37 (17.73); $LuOH^{2+}$ / 0.35 (16.73). The occurrence of these reactions indicates that $PA(MO^+) \leq PA(H_2O)$ = 691 kJ mol^{-1}; in view of the activation barriers typically associated with such charge-separation processes, it can be assumed that $PA(MO^+) < PA(H_2O)$ by at least ~100 kJ mol^{-1}. For comparison, the proton affinity of LaO^+ has been estimated as 482 kJ mol^{-1} (45), which although is remarkably high for a cation is still some ~200 kJ mol^{-1} lower than $PA(H_2O)$.

Electron transfer reactions of MO^{2+}: An evaluation of IE(CmO^+) and IE(LnO^+) (Ln = La, Gd, Lu)

Reactions of four MO^{2+} ions (M = Cm, La, Gd, Lu) with N_2O revealed that oxidation of them did not occur. This contrasts with the behavior of UO^{2+} (13,46), NpO^{2+} (13), PuO^{2+} (13), and PaO^{2+} (14), each of which is efficiently ($k/k_{COL} \geq 0.19$) oxidized by N_2O to the corresponding dipositive actinyl ion, AnO_2^{2+}. The behavior of CmO^{2+} and these three LnO^{2+} ions (Ln = La, Gd, Lu) is instead reminiscent of that of ThO^{2+} (13), which is similarly not oxidized by N_2O. The absence of oxidation to MO_2^{2+} by N_2O reflects a common characteristic of these metals in their resistance to form oxidation states as high as M(VI), which is the formal oxidation state in a MO_2^{2+} ion. In contrast to ThO^{2+}, and other early AnO^{2+} ions (13), the electron affinities of the four MO^{2+} ions studied in the

present work are sufficiently high that facile electron transfer from N_2O produces the MO^+ ions.

We previously employed electron transfer (ET) from dipositive ions to neutrals, Equation 5a where "M^{2+}" is a bare or oxo-ligated metal ion and R is a diatomic or triatomic molecule, to estimate ionization energies, and this approach has been described in detail elsewhere (13,14).

$$M^{2+} + R \rightarrow M^+ + R^+ \quad (5a)$$

$$\Delta_r H^{ET} = IE(R) - EA(M^{2+}) = IE(R) - IE(M^+) \quad (5b)$$

Whereas electron transfer from a neutral to a monopositive ion is generally facile, electron transfer from neutrals to dipositive ions usually exhibits substantial activation barriers. After the onset of electron transfer, its efficiency generally increases with increasing exothermicity. The thermodynamic onset threshold and relative rates for electron transfer can be used to estimate comparative electron affinities of dipositive ions. A "curve-crossing" model has been employed to describe electron transfer to multiply charged ions from neutrals (47-50). According to this description, electron transfer from a neutral R to a dipositive M^{2+} (Eqn. 5a) will occur if the attractive M^{2+}-R and repulsive M^+-R^+ potential energy curves cross at a sufficiently short distance for resonant electron hopping; this distance is in the approximate range of 0.2 – 0.6 nm (48). The maximum curve crossing distance for electron transfer corresponds to a minimum exothermicity for the onset of transfer, $-\Delta_r H^{ET}$ (47,50). Accordingly, the onset of transfer can be used to estimate the difference between the electron affinity of M^{2+} and the ionization energy of R; i.e., $-\Delta_r H^{ET}(\text{mimimum}) = EA(M^{2+}) - IE(R)$ where the

minimum enthalpy corresponds to the initial appearance of transfer. Close to the thermodynamic threshold for resonant electron transfer, it is reasonable to presume that the M^+ and R^+ products have minimal internal and translational energies. Favorable alternative reaction pathways can obscure electron transfer onset, as was noted in the preceding section for the reactions of Cm^{2+} and Gd^{2+} with ethylene oxide where electron transfer is substantially exothermic but is not observed because formation of the MO^+ charge-separation products is much more exothermic. To avoid the potential complication of competing exit channels, electron transfer studies are preferably carried out with ion-neutral pairs which do not otherwise react with one another. The electron transfer investigations reported here are phenomenological and the interpretation of the results is based on comparisons with measured efficiencies for ion-neutral pairs for which $\Delta_r H^{ET}$ is known. This method for estimating unknown $EA(M^{2+})$ (= $IE(M^+)$) is qualitative, as is reflected in the rather large assigned uncertainties, ±0.4 eV.

The efficiencies for electron-transfer from neutral molecules to the dipositive metal oxide ions, CmO^{2+}, LaO^{2+}, GdO^{2+} and LuO^{2+}, were used to estimate the $EA(MO^{2+})$ = $IE(MO^+)$. The measured electron-transfer kinetics for these MO^{2+} ions are given in Table 7. Estimates for the $IE(MO^+)$ are based on comparison with electron-transfer efficiencies for selected bare "calibration" M^{2+} ions (M = Sn, Pb, Mn, Ge, Bi). These latter efficiencies for the "calibration" M^{2+} ions, reported previously (13,14), are summarized in Table 8. The results in Table 8 suggest that the thermodyanmic onset for electron transfer occurs in the approximate range of 1 eV (from the Pb^{2+}/CO reaction) and 1.2 eV (from the Pb/CO_2 reaction), which is in accord with the estimate of ~1 eV given by Roth and Freiser (50).

From a comparison of the relative k/k_{COL} values for the MO^{2+} ions (Table 7) and M^{2+} ions (Table 8), we arrive at the following ordering of second ionization energies:

$$Mn^{+} < CmO^{+} < LaO^{+} < Ge^{+} < GdO^{+} \approx LuO^{+} << Bi^{+}$$

The results with CO in particular suggest that the four IE(MO^{+}) are fairly close to IE(Mn^{+}) = 15.64 eV and IE(Ge^{+}) = 15.92 eV. We arrive at the following estimates: IE(CmO^{+}) = 15.8±0.4 eV; IE(LaO^{+}) = 15.9±0.4 eV; IE(GdO^{+}) = 16.0±0.4 eV; IE(LuO^{+}) = 16.0±0.4 eV. As remarked above, the relatively large assigned uncertainties for these values reflect the qualitative nature of the method.

A somewhat lower value of IE(LaO^{+}) = 15.2±0.4 eV was previously estimated from charge-stripping experiments (45). However, a recent re-evaluation of the charge-stripping method by Roithová and Schröder indicates that earlier IE assignments from these types of experiments should generally be revised (51).

We can now estimate the dissociation energies of MO^{2+} to {M^{2+} + O} using Eqn. (6):

$$D(M^{2+}\text{-}O) = D(M^{+}\text{-}O) + IE(M^{+}) - IE(MO^{+}) \qquad (6)$$

Employing the D(M^{+}-O) derived above and D(La^{+}-O) = 847±15 kJ mol^{-1} from ref. (34) (we assign a greater uncertainty of ±30 kJ mol^{-1} to this latter value); the IE(M^{+}) in Table 1 and IE(La^{+}) = 11.06 eV from ref. (17); and the IE(MO^{+}) values obtained here, we arrive at the following: D(Cm^{2+}-O) = 342±55 kJ mol^{-1}; D(La^{2+}-O) = 388±50 kJ mol^{-1}; D(Gd^{2+}-O) = 403±50 kJ mol^{-1}; and D(Lu^{2+}-O) = 357±50 kJ mol^{-1}. The estimated dissociation energy for GdO^{2+} in particular suggests that the oxidation of Gd^{2+} to GdO^{2+} by C_2H_4O should be somewhat exothermic; as noted in Table 6, this oxidation process was not observed. Even if oxidation to {GdO^{2+} + C_2H_4} is thermodynamically allowed, the observed {GdO^{+}

+$C_2H_4^+$} exit channel is energetically favored because IE(C_2H_4) = 10.51 eV is more than 5 eV below IE(GdO^+) = 16.0±0.4 eV. It should be noted that if IE(M^+) > IE(O) = 13.62 eV, then dissociation to {$M^+ + O^+$} is energetically (but not necessarily kinetically) favored over dissociation to {$M^{2+} + O$}; i.e., D(M^+-O^+) < D(M^{2+}-O). This latter thermodynamic condition evidently applies to LuO^{2+} given the unusually large value of IE(Lu^+) = 13.90 eV: D(Lu^+-O^+) = D(Lu^{2+}-O) - 0.28 eV = 330±50 kJ mol^{-1}.

Catalytic oxidation of CO by N_2O mediated by MO^{2+} (M = Cm, La, Gd, Lu)

The D(M^{2+}-O) vaues derived above, in the range of 342-403 (±50) kJ mol^{-1}, are each intermediate between D(N_2-O) = 167 kJ mol^{-1} and D(CO-O) = 532.2 kJ mol^{-1}, and thus satisfy the thermodynamic requirement for catalytic oxygen-transfer from N_2O to CO by MO^{2+}: D(N_2-O) < D(M^{2+}-O) < D(CO-O). It was found experimentally that the four M^{2+} ions—M = Cm, La, Gd and Lu—each catalyze the gas-phase oxidation of CO by N_2O, according to the sequential O-atom transport reactions (7) and (8):

$$M^{2+} + N_2O \rightarrow MO^{2+} + N_2 \qquad (7)$$

$$MO^{2+} + CO \rightarrow M^{2+} + CO_2 \qquad (8)$$

The net reaction for the catalytic cycles is given by Eqn (9) = (7) + (8):

$$N_2O + CO \rightarrow N_2 + CO_2 \qquad (9)$$

The catalytic cycles are summarized in Scheme 2, where M = Cm, La, Gd, Lu. These cycles were explicitly demonstrated by the procedure described in detail previously for the analogous catalytic cycle mediated by PaO_2^{2+} (14). Briefly, the M^{2+} ions were exposed to a mixture of N_2O and CO, the MO^{2+} product from Eqn. (7) was isolated, and the subsequent kinetics were monitored. The concurrent in-growth of M^{2+}—Eqn. (8)—and regeneration of MO^{2+}—Eqn. (7)—was confirmed by a positive deviation from

pseudo-first order kinetics for the depletion of MO^{2+}, which demonstrated the regeneration of the MO^{2+} ion, and thus that both Eqns. (7) and (8) were occurring simultaneously. The result is the overall cycle shown in Scheme 2.

However, the catalytic cycle for each of the four MO^{2+} ions is poisoned by depletion of the MO^{2+} oxygen-atom carriers according to the electron-transfer Eqns. (10) and (11):

$$MO^{2+} + N_2O \rightarrow MO^{+} + N_2O^{+} \quad (10)$$

$$MO^{2+} + CO \rightarrow MO^{+} + CO^{+} \quad (11)$$

The kinetics for Eqns. (7), (10) and (11) are given in Tables 6 and 7. The kinetics for Eqn. (8), given as efficiencies, k/k_{COL}, and as $k/10^{-10}$ cm^3 $molecule^{-1}$ s^{-1} in brackets, are as follows: CmO^{2+} / 0.26 (3.54); LaO^{2+} / 0.21 (2.94); GdO^{2+} / 0.16 (2.23); and LuO^{2+} / 0.17 (2.30). Electron-transfer from N_2O to the MO^{2+}, to produce inert MO^{+}, proceeds efficiently—$k/k_{COL} \geq$ 0.38 (Table 7)—and the catalytic cycles are thus quenched rapidly.

From energetic considerations alone, observation of the exit channel corresponding the right side of Eqn. (8), rather than the charge-separation channel to give $\{M^{+} + CO_2^{+}\}$, would suggest that $IE(M^{+}) \leq IE(CO_2) = 13.78$ eV; in the case of M = Lu, this implication is inconsistent with the literature value, $IE(Lu^{+}) = 13.90$ eV (17). However, as discussed above, barriers to formation of two monopositive ions from a dipositive ion can be sufficiently large such that energetically favorable charge-separation processes may be so kinetically hindered as to not appear.

Summary and Conclusions

A central goal of the work reported here was to derive thermodynamic estimates for curium oxide molecules based on the kinetics of oxidation, electron-transfer, and diene activation reactions of the bare and oxo-ligated curium cations.

The thermodynamic quantities derived in the present work for curium and lanthanide oxides are compiled in Table 9. For the curium oxide molecules, the only value determined previously for comparison is D(Cm-O) ≈ 728 kJ mol^{-1} from Smith and Peterson (5), which is in good agreement with our value. A recent theoretical value of D(Cm-O) ≈ 685 kJ mol^{-1} (9) is also in remarkably good accord. Our suggested values for D(Gd^+-O) and D(Lu^+-O) in Table 9 are slightly higher than literature values (34); values are not available for comparison with our IE(LnO^+) or D(Ln^{2+}-O) (Ln = La, Gd, Lu).

The D(M^{2+}-O) (M = Cm, La, Gd and Lu) are intermediate between D(N_2-O) and D(OC-O), which is the thermodynamic requirement for O-atom transport from N_2O to CO. It was demonstrated that each of these four MO^{2+} do indeed catalyze the oxidation of CO to CO_2 concomitant with the reduction of N_2O to N_2. There are several examples of such gas-phase oxidation/reduction couples mediated by monopositive metal oxide ions (52), but apparently PaO_2^{2+} is the only dipositive oxide ion to have been shown previously to exhibit such catalytic behavior (14).

Oxidation of CmO^+ did not occur under with thermalized states. However, CmO^+ produced from the oxidation of Cm^+ by O_2 was further oxidized to CmO_2^+ in the absence of collisional de-excitation. This oxidation is attributed to a thermodynamically and/or kinetically hindered oxidation which proceeds via an excited state CmO^{+*}. This demonstrates that CmO_2^+ is a stable albeit elusive species.

Acknowledgements

This work was sponsored by Fundação para a Ciência e a Tecnologia (FCT) and POCI 2010 (cofinanced by FEDER) under contract POCI/QUI/58222/2004; and by the Director, Office of Science, Office of Basic Energy Sciences, Division of Chemical Sciences,

Geosciences and Biosciences of the U.S. Department of Energy under Contracts DE-AC05-00OR22725 at ORNL, and DE-AC02-05CH11231 at LBNL. M.S. is grateful to FCT for a Ph.D. grant.

References

1) J.K. Gibson, *Int. J. Mass Spectrom.* **2001,** *214***,** 1-21.

2) J.K. Gibson, J, Marçalo, *Coord. Chem Rev.* **2006**, *250*, 776-783.

3) D.L. Hildenbrand, L.V. Gurvich, V.S. Yungman, *The Chemical Thermodynamics of Actinide Elements and Compounds. Part 13: The Gaseous Actinide Ions,* IAEA: Vienna, 1985.

4) R.J.M. Konings, L.R. Morss, J. Fuger, in *The Chemistry of the Actinide and Transactinide Elements, Third Ed.*, Edited by L.R. Morss, N.M. Edelstein, J. Fuger, Springer: Dordrecht, 2006, pp. 2113-2224.

5) P.K. Smith, D.E. Peterson, *J. Chem. Phys.* **1970**, *52*, 4963-4972.

6) R.G. Haire, *J. Alloys Compd.*, **1994**, *213/214*, 185-190.

7) J.P. Hiernaut, C. Ronchi, *J. Nucl. Mat.* **2004**, *334*, 133-138.

8) R.J.M. Konings, *J. Nucl. Mat.* **2001**, *298*, 255-268.

9) A. Kovács, R.J.M. Konings, J. Raab, L. Gagliardi, *Phys. Chem. Chem. Phys.*, **2008**, *10*, 1114-1117.

10) M. Santos, J. Marçalo, A. Pires de Matos, J.K. Gibson, R.G. Haire, *J. Phys. Chem. A* **2002**, *106*, 7190-7194.

11) M. Santos, J. Marçalo, J.P. Leal, A. Pires de Matos, J.K. Gibson, R.G. Haire, *Int. J. Mass Spectrom.* **2003**, *228*, 457-465

12) J.K. Gibson, R.G. Haire, J. Marçalo, M. Santos, A. Pires de Matos, J.P. Leal, *J. Nucl. Mat.* **2005**, *344*, 24-29.

13) J.K. Gibson, R.G. Haire, J. Marçalo, M. Santos, A. Pires de Matos, *J. Phys. Chem. A* **2005**, *109*, 2768-2781.

14) M. Santos, A. Pires de Matos, J. Marçalo, J.K. Gibson, R.G. Haire, R. Tyagi, R.M. Pitzer, *J. Phys. Chem. A* **2006**, *110*, 5751-5759.

15) H.H. Cornehl, R. Wesendrup, J.N. Harvey, H. Schwarz, *J. Chem. Soc., Perkin Trans. 2* **1997**, 2283-2291.

16) J. Blaise, J.-F. Wyart, *Energy Levels and Atomic Spectra of Actinides*; Tables Internationales de Constantes, Université Pierre et Marie Curie: Paris, 1992 (http://www.lac.u-psud.fr/Database/Contents.html)

17) W.C. Martin, R. Zalubas, L. Hagan, *Atomic Energy Levels—The Rare Earth Elements*; U.S. Department of Commerce: Washington, D.C., 1978.

18) L.R. Morss in *The Chemistry of the Actinide Elements, 2nd Ed.*, J.J. Katz, G.T. Seaborg, L.R. Morss, Eds.; Chapman and Hall: London, 1986; Chap. 17, pp. 1278-1360.

19) J. Marçalo, J.P. Leal, A. Pires de Matos, *Int. J. Mass Spectrom. Ion Processes* **1996**, *157/158*, 265-274.

20) J. Marçalo, J.P. Leal, A. Pires de Matos, A.G. Marshall, *Organometallics* **1997**, *16*, 4581-488.

21) D.D. Perrin; W.L.F. Armarego, *Purification of Laboratory Chemicals,* 3rd Ed.; Pergamon Press: Oxford, 1988.

22) J.E. Bruce, J.R. Eyler, *J. Am. Soc. Mass Spectrom.* **1992**, *3*, 727-733.

23) Y. Lin, D.P. Ridge, B. Munson, *Org. Mass Spectrom.* **1991**, *26*, 550-558.

24) J.E. Bartmess, R.M. Georgiadis, R.M. *Vacuum* **1983**, *33*, 149-153.

25) D.R. Lide, Ed. *CRC Handbook of Chemistry and Physics*, 75th ed., CRC Press: Boca Raton, 1994.

26) S. Guan, A.G. Marshall, *Int. J. Mass Spectrom. Ion Processes* **1996**, *157/158*, 5-37.

27) T. Su, W.J. Chesnavich, *J. Chem. Phys.* **1982**, *76*, 5183-5185.

28) S.G. Lias, J.E. Bartmess, J.F. Liebman, J.L. Holmes, R.D. Levin, W.G. Mallard, *Gas-Phase Ion and Neutral Thermochemistry*; American Chemical Society: Washington, D.C., 1988.

29) NIST Chemistry WebBook – NIST Standard Reference Database Number 69, Eds. P.J. Linstrom and W.G. Mallard, June 2005, National Institute of Standards and Technology, Gaithersburg MD, 20899 (http://webbook.nist.gov).

30) P. Cheng, G.K. Koyanagi, D.K. Bohme, *J. Phys. Chem. A* **2001**, *105*, 8964-8968.

31) V. Blagojevic, E. Flaim, M.J.Y. Jarvis, G.K. Koyanagi, D.K. Bohme, *Int. J. Mass Spectrom.* **2006**, *249-250*, 385-391.

32) P. Cheng, G.K. Koyanagi, D.K. Bohme, *ChemPhysChem* **2006**, *7*, 1813-1819.

33) P. Cheng, G.K. Koyanagi, D.K. Bohme, *J. Phys. Chem. A* **2006**, *110*, 12832-12838.

34) M.S. Chandrasekharaiah, K.A Gingerich in *Handbook on the Chemistry and Chemistry of Rare Earths*, K. A. Gschniedner, Jr., L. Eyring, Eds.; Elsevier: Amsterdam, 1989; Volume 12, Chapter 86.

35) J. Han, L.A. Kaledin, V. Goncharov, A.V. Komissarov, M.C. Heaven, *J. Am. Chem. Soc.* **2003**, *125*, 7176-7177.

36) A.J. Gaunt, S.D. Reilly, A.E. Enriquez, B.L. Scott, J.A. Ibers, P. Sekar, K.I.M. Ingram, N. Kaltsoyannis, M.P. Neu, *Inorg. Chem.* **2008,** *47*, 29-41.

37) J.K. Gibson, R.G. Haire, J. Marçalo, M. Santos, A. Pires de Matos, M.K. Mrozik, R.M. Pitzer, B.E. Bursten, *Organometallics* **2007**, *26*, 3947-3956.

38) V. Goncharov, M.C. Heaven, *J. Chem. Phys.* **2006**, *124*, 64312-1-7.

39) J.K. Gibson, R.G. Haire, *J. Phys. Chem. A* **1998**, *102*, 10746-10753.

40) N. Erdmann, M. Nunnemann, K. Eberhardt, G. Hermann, G. Huber, S. Köhler. J.V. Kratz, G. Passler, J.R. Peterson, N. Trautmann, A. Waldek, *J. Alloys Compds.* **1998**, *271-273*, 837-840.

41) J.K. Gibson, *J. Phys. Chem. A* **2003**, *107*, 7891-7899.

42) L. Brewer, *J. Opt. Soc. Am.* **1971**, *61*, 1666-1682.

43) S. Petrie, J. Wang, D.K. Bohme, *Chem. Phys. Lett.* **1993**, *204*, 473-480.

44) J.L. Elkind, L.S. Sunderlin, P.B. Armentrout, *J. Phys. Chem.* **1989**, *93*, 3151-3158.

45) D. Schröder, H. Schwarz, J.N. Harvey, *J. Phys. Chem. A* **2000**, *104*, 11257-11260.

46) H.H. Cornehl, C. Heinemann, J. Marçalo, A. Pires de Matos, H. Schwarz, *Angew. Chem. Int. Ed. Engl.* **1996**, *35*, 891-894.

47) R. Tonkyn, J. C. Weisshaar, *J. Am. Chem. Soc.* **1986**, *108*, 7128-7130.

48) J.R. Gord, B.S. Freiser, S.W. Buckner, *J. Chem. Phys.* **1991**, *94*, 4282-4290.

49) J.R. Gord, B.S. Freiser, S.W. Buckner, *J. Phys. Chem.* **1991**, *95*, 8274-8279.

50) L.M. Roth, B.S. Freiser, *Mass Spectrom. Rev.* **1991**, *10*, 303-328.

51) J. Roithová, D. Schröder, *Int. J. Mass Spectrom.* **2007**, *267*, 134-138.

52) D.K. Böhme, H. Schwarz, *Angew. Chem. Int. Ed.* **2005**, *44*, 2236-2254.

Table 1 - Energetics of monopositive metal ions [a]

	Ground-State Configuration	Excited Reactive-State Configuration(s) (Excitation energy given in brackets [b])	IE(M^+) (ev) [c]
Cm^+	$5f^7 7s^2$	$5f^7 6d7s$ (0.50 eV); $5f^7 6d^2$ (1.84 eV)	12.4
Gd^+	$4f^7 5d6s$	$4f^7 5d^2$ (0.50 eV)	12.09
Lu^+	$4f^{14} 6s^2$	$4f^{14} 5d6s$ (1.46 eV); $4f^{14} 5d^2$ (3.64 eV)	13.90

[a] The closed shell Xe and Rn core electronic configurations are not included. The energies for Cm^+ are from ref. (16); those for Gd^+ and Lu^+ are from ref. (17).

[b] 1eV = 96.485 kJ mol^{-1}

[c] Value for Cm^+ from ref. (18); values for Gd^+ and Lu^+ are from ref. (17)

Table 2 - Reaction products and kinetics for M^+ ions with oxidants[a]

	N_2O	C_2H_4O	H_2O	O_2	CO_2	NO	CH_2O
Cm^+	CmO^+ 0.17 (1.20)	CmO^+ 0.26 (4.49)	CmO^+ 0.049 (1.07)	CmO^+ 0.37 (2.03)	CmO^+ 0.080 (0.53)	CmO^+ 0.013 (0.081)	NR
Gd^+	GdO^+ 0.46 (3.32)	GdO^+ 0.32 (5.64)	GdO^+ 0.089 (2.11)	GdO^+ 0.61 (3.47)	GdO^+ 0.22 (1.46)	GdO^+ 0.16 (1.02)	GdH_2^+ (55) GdO^+ (25) $GdOCH_2^+$ (20) 0.088 (2.12)
Lu^+	LuO^+ 0.21 (1.48)	LuO^+ (85) $LuOH^+$ (10) $LuOH_2^+$ (5) 0.35 (6.08)	LuO^+ 0.033 (0.79)	LuO^+ 0.12 (0.66)	LuO^+ 0.013 (0.09)	NR	NR

[a] Where more than one product was observed the relative yields are given in parentheses as percentages. The pseudo-first-order rates are expressed as reaction efficiencies, k/k_{COL}, and in brackets as the absolute rates, $k/10^{-10}$ $cm^3 molecule^{-1}$ s^{-1}. The absolute rates are considered to be accurate to within ±50%, and the relative values for comparative purposes to within ±20%. "NR" indicates no reaction within the detection limit: $k < 1 \times 10^{-12}$ cm^3 $molecule^{-1}$ s^{-1} ($k/k_{COL} < 0.001$).

Table 3 - Bond dissociation energies and ionization energies of reagent molecules (RO) [a]

	BDE(R-O) / kJ mol^{-1}	IE(RO) / eV
N_2O	167.1(1)	12.89(0)
C_2H_4O	354.3(6)	10.56(1)
H_2O	491.0(1)	12.62(0)
O_2	498.4(1)	12.07(0)
CO_2	532.2(2)	13.78(0)
NO	631.6(4)	9.26(0)
CH_2O	751.5(1)	10.88(1)
CO	1076.4(1)	14.01(0)

[a] BDEs are from ref. (28); IEs are from ref. (29). The uncertainty in the final figure is in parentheses.

Table 4 – Reaction products and kinetics for MO^+ and Cm^+ with butadiene and isoprene [a]

	1,3-C_4H_6	C_5H_8
CmO^+	NR	$CmOC_3H_4^+$ (50) $CmOC_5H_6^+$ (50) 0.19 (1.96)
GdO^+	NR	$GdOC_3H_4^+$ (60)

		$GdOC_5H_6^+$ (40) 0.11 (1.24)
LuO^+	$LuOC_2H_2^+$ (50) $LuOC_2H_4^+$ (35) $LuOC_4H_4^+$ (15) 0.20 (2.14)	$LuOC_3H_4^+$ (50) $LuOC_5H_6^+$ (50) 0.33 (3.50)
Cm^+	$CmC_2H_2^+$ (85) $CmC_4H_4^+$ (5) $CmC_4H_6^+$ (10) 0.18 (1.84)	$CmC_2H_2^+$ (20) $CmC_3H_4^+$ (50) $CmC_5H_6^+$ (30) 0.22 (2.27)

[a] Results are presented as described in footnote (a) of Table 3.

Table 5 - Ionization energies and proton affinities of selected neutrals [a]

	IE/eV	PA/eV
C_5H_8 (isoprene)	8.86	8.56
C_4H_6 (1,3-butadiene)	9.07	8.12
C_4H_8 (1-butene)	9.55	NA
C_3H_6 (propene)	9.73	7.79
C_2H_4 (ethylene)	10.51	7.05

C_2H_4O (ethylene oxide)	10.56	8.02
H_2O (water)	12.62	7.16

[a] Ionization energies (IE) and proton affinities (PA) are from ref. (29)

Table 6 – Reaction products and kinetics for M^{2+} with oxidants

	N_2O [b]	C_2H_4O	H_2O	O_2	CO_2	NO	CH_2O
Cm^{2+}	CmO^{2+} 0.22 (2.99)	CmO^{+} 0.26 (8.98)	$CmOH^{2+}$ 0.027 (1.17)	NR	NR	Cm^{+} 0.29 (3.61)	CmO^{+} 0.013 (0.58)
Gd^{2+}	GdO^{2+} 0.35 (5.11)	GdO^{+} 0.28 (9.80)	$GdOH^{2+}$ 0.098 (4.66)	NR	NR	Gd^{+} 0.28 (3.53)	GdH^{+} (65) GdO^{+} (35) 0.12 (5.79)
Lu^{2+}	LuO^{2+} 0.29 (4.12)	Lu^{+} (30) LuO^{+} (70) 0.27 (9.52)	$LuOH^{2+}$ 0.10 (4.87)	NR	NR	Lu^{+} 0.31 (3.96)	Lu^{+} (65) LuH^{+} (35) 0.23 (10.89)

[a] The results are presented as described in footnote (a) of Table 3.

[b] The La^{2+}/N_2O reaction produced LaO^{2+} with the following kinetics: $k/k_{COL} = 0.31$; $k = 4.47 \times 10^{-10}$ cm^3 $molecule^{-1}$ s^{-1}.

Table 7 – Electron transfer kinetics for MO^{2+} [a]

	N_2O (12.89 eV)	CO_2 (13.78 eV)	CO (14.01 eV)
CmO^{2+}	0.38 (5.29)	0.066 (0.86)	0.020 (0.27) [b]
LaO^{2+}	0.38 (5.53)	0.13 (1.74)	0.020 (0.27) [b]
GdO^{2+}	0.47 (6.73)	0.20 (2.66)	0.050 (0.68)
LuO^{2}	0.51 (7.20)	0.40 (5.32)	0.041 (0.55)

$^{+}$			

[a] In each case the product was MO^+ (+ RO^+). The kinetics are presented as described in footnote (a) of Table 2. The IEs of the neutrals from Table 3 are given in parentheses. Reactions of the four MO^{2+} with N_2 (IE = 15.58 eV) and Ar (IE = 15.76 eV) were also studied and no electron transfer reactions were detected.
[b] The dominant reaction channels for CmO^{2+} and LaO^{2+} with CO were O-atom transfer to give M^{2+} and CO_2. As a result, the derived minor contributions for the electron transfer channels from CO to CmO^{2+} and LaO^{2+} have a larger uncertainty than is typical (i.e., > 50%).

Table 8 – Electron transfer kinetics for dipositive metal ions [a]

	IE(M^+)	N_2O (12.89 eV)	CO_2 (13.78 eV)	CO (14.01 eV)
Sn^{2+}	14.63 eV	0.01 {1.74 eV}	NR {0.85 eV}	NR {0.62 eV}
Pb^{2+}	15.03 eV	0.11 {2.14 eV}	0.008 {1.25 eV}	0.002 {1.02 eV}
Mn^{2+}	15.64 eV	0.44 {2.75 eV}	0.014 {1.86 eV}	0.017 {1.63 eV}
Ge^{2+}	15.93 eV	0.55 {3.04 eV}	0.22 {2.15 eV}	0.027 {1.92 eV}
Bi^{2+}	16.69 eV	0.40 {3.80 eV}	0.34 {2.91 eV}	0.24 {2.68 eV}

[a] The electron transfer efficiencies, k/k_{COL}, are from refs. (13,14). The IE(M^+) are from ref. (25). The IE(RO) given in parentheses are from ref. (29). The exothermicities for electron transfer from RO to M^{2+} (IE(M^+) – IE(RO)) are given in brackets.

Table 9 – Thermodynamics of metal oxide molecules [a]

	IE(MO)	IE(MO^+)	D(M-O)	D(M^+-O)	D(M^{2+}-O)
Cm	6.4±0.2	15.8±0.4	710±45	670±40	342±55
La	ND	15.9±0.4	ND	ND	388±50
Gd	ND	16.0±0.4	ND	780±30	403±50

Lu	ND	16.0±0.4	ND	560±30	357±50

[a] These thermodynamic values were derived from the experimental results reported here; "ND" indicates that this quantity was not determined in the present work. The ionization energies (IE) are in units of eV; the bond dissociation energies (D) are in units of kJ mol^{-1} (1 eV = 96.485 kJ mol^{-1}).

Scheme 1 – Postulated mechanism for dehydrogenation of ethylene oxide by MO^+

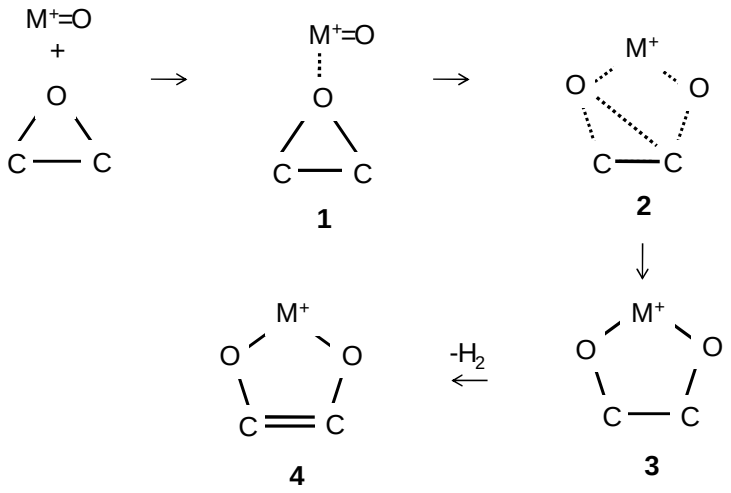

Scheme 2 – Catalytic oxidation of CO by N_2O mediated by MO^{2+} (M = Cm, La, Gd, Lu)